

Faraday rotation and sensitivity of (100) bismuth-substituted ferrite garnet filmsL. E. Helseth, A. G. Solovyev, R. W. Hansen, E. I. Il'yashenko, M. Baziljevich, and T. H. Johansen
Department of Physics, University of Oslo, P.O. Box 1048 Blindern, N-0316 Oslo, Norway

(Received 17 February 2002; published 2 August 2002)

We have investigated the Faraday rotation of in-plane magnetized bismuth-substituted ferrite garnet films grown by liquid phase epitaxy on (100) oriented gadolinium gallium garnet substrates. The Faraday spectra were measured for photon energies between 1.7 and 2.6 eV. To interpret the spectra, we use a model based on two electric dipole transitions: one tetrahedral and one octahedral. Furthermore, the Faraday rotation sensitivity was measured at 2.3 eV, and found to be in good agreement with the theoretical predictions. In particular, we find that the sensitivity increases linearly with the bismuth content and nonlinearly with the gallium content.

DOI: 10.1103/PhysRevB.66.064405

PACS number(s): 78.20.Ls, 75.70.Ak

I. INTRODUCTION

It is well known that bismuth-substituted ferrite garnets (Bi:FG's) have a giant magneto-optical response.¹⁻⁹ For this reason, they have found widespread use as optical switchers, optical isolators, and magnetic-field sensors. Some years ago it was realized that Bi:FG films with in-plane magnetization allow effective visualization and detection of magnetic fields.^{10,11} This discovery triggered a large number of quantitative studies of magnetic fields from superconductors, domain formation in magnetic materials, currents in microelectronic circuits, and recorded patterns in magnetic storage media.¹²⁻¹⁷ However, no systematic studies have been carried out to characterize the magneto-optic properties of these films. Of particular interest here is the Faraday rotation, since this parameter determines the usefulness of the indicator.

Bi:FG films grown on (100) oriented substrates have been shown to have a number of unique properties which make them excellent candidates for magneto-optic imaging. First, these films exhibit very little domain activity, and respond to an increasing external field by a continuous rotation of the magnetization vector. Second, the sensitivity of the films is easily tuned by altering the chemical composition. The sensitivity of the Faraday rotation to an external field is of major importance in magneto-optic imaging and detection, in particular when the external field is weak. To date, several studies have been done to determine the sensitivity of bulk-samples and (111) oriented Bi:FG films.¹⁸⁻²²

In a previous paper we presented an experimental and theoretical study of the Faraday rotation at saturation.²³ In that study a very simple model based on two electric dipole transitions, one tetrahedral and one octahedral, was used to explain the experimental data. Here we extend the work in that paper, and also introduce several different features. We have grown a series of gallium-substituted Bi:FG films using the liquid phase epitaxy (LPE) technique, and characterized their chemical composition. The Faraday rotation spectra have been measured for photon energies between 1.7 and 2.6 eV, corresponding to wavelengths between 730 and 480 nm. It is shown that the Faraday rotation changes significantly with the amount of substituted gallium and bismuth. Furthermore, the comparison of experimental and theoretical data confirms that the magneto-optic response increases linearly with the bismuth substitution and decreases almost linearly

with the gallium substitution. We also report experimental data for the sensitivity of these materials, and find that the sensitivity depends nonlinearly on the gallium substitution, in good agreement with the theoretical model.

II. SAMPLE PREPARATION

Single-crystal films of Bi:FG were grown by isothermal LPE (about 700 °C) from Bi₂O₃/PbO/B₂O₃ flux onto (100) oriented gadolinium gallium garnet (GGG) substrates. The growth takes place while the substrate is dipped into the melt contained in a Pt crucible. During the growth, the parameters could be controlled to create low magnetic coercivity and in-plane magnetization in the garnet films. The thickness of the films was measured using a scanning electron microscope (SEM) and confirmed with optical techniques, while their composition were determined with an electron microprobe (EMP). Thicknesses and compositions of the selected samples are listed in Table I.

From Table I one sees that the films can be represented by the following general formula: {Re_{3-x}Bi_x}[Fe_{2-z_a}Ga_{z_a}]₁₂ × (Fe_{3-z_d}Ga_{z_d})O₁₂, where { } indicates the dodecahedral site, [] the octahedral site, and () the tetrahedral site. Note that only the total gallium content $z = z_a + z_d$ can be extracted from the EMP, and to determine z_a and z_d separately other techniques such as neutron spectroscopy must be applied. The distribution of gallium on tetrahedral and octahedral sites have been examined in a number of studies on garnets with and without bismuth.²⁴⁻²⁶ These results indicate that around 90% of the gallium occupies the tetrahedral site. This fact will be used later in this paper.

The films also contain small amounts of Pb, typically of the order of 0.05. Although Pb is well known to give a substantial increase in the magneto-optic effect, the Pb content is here so small that it does not influence the Faraday rotation significantly. We will therefore neglect it.

III. FARADAY ROTATION SPECTRA

We have measured the Faraday spectra (at room temperature and saturation) of the films presented in Table I. Shown in Figs. 1 and 2 is the observed Faraday rotation as a function of wavelength for samples 7 and 8, respectively. Note that both films have maximum rotation near 2.45 eV, a fea-

TABLE I. The thickness and chemical composition of the samples.

Sample	Lu	Y	Tm	Bi	Fe	Ga	$t(\mu\text{m})$
1	2.5	0	0	0.5	4.9	0.1	4.0
2	2.4	0	0	0.6	4.8	0.2	3.5
3	2.3	0	0	0.7	4.7	0.3	3.5
4	2.3	0	0	0.7	4.4	0.6	4.0
5	2.3	0	0	0.7	4.2	0.8	4.0
6	2.4	0	0	0.6	4.1	0.9	3.3
7	0	0	2.3	0.7	4.1	0.9	3.5
8	1.4	1	0	0.6	4.1	0.9	4.0
9	2.2	0	0	0.8	3.8	1.2	2.6
10	2.2	0	0	0.8	3.9	1.1	4.0
11	2.1	0	0	0.9	3	1	4.0
12	1.6	0.7	0	0.7	3.8	1.2	7.5

ture characteristic of all the films considered in this study. In fact, all the films exhibit the same spectral shape, with only minor deviations from that seen in Figs. 1 and 2.

In order to understand the behavior of the spectra, we have adopted the theory developed in Refs. 23, 27, and 28. Here the expression for the Faraday rotation is given by

$$\Theta_F^{sat} = \frac{\pi e^2 \omega^2}{nmc} \sum_{i=a,d} \frac{Nf_i}{\omega_i} \left\{ \frac{(\omega_i + \Delta_i)^2 - \omega^2 - \Gamma_i^2}{[(\omega_i + \Delta_i)^2 - \omega^2 + \Gamma_i^2]^2 + 4\omega^2 \Gamma_i^2} - \frac{(\omega_i - \Delta_i)^2 - \omega^2 - \Gamma_i^2}{[(\omega_i - \Delta_i)^2 - \omega^2 + \Gamma_i^2]^2 + 4\omega^2 \Gamma_i^2} \right\}, \quad (1)$$

where ω_i represent the resonance energy, Δ_i the spin orbit splitting energy, f_i the oscillator strength, while Γ_i is the half linewidth of the transition. Furthermore, e and m are the electron charge and mass, respectively, whereas N is the active ion density.

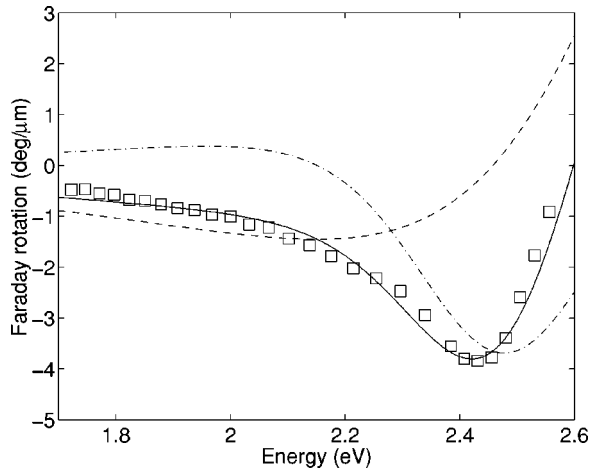


FIG. 1. The Faraday rotation as a function of wavelength for sample 7. The dashed line is the contribution from the octahedral transition, whereas the dash-dotted line is due to the tetrahedral contribution.

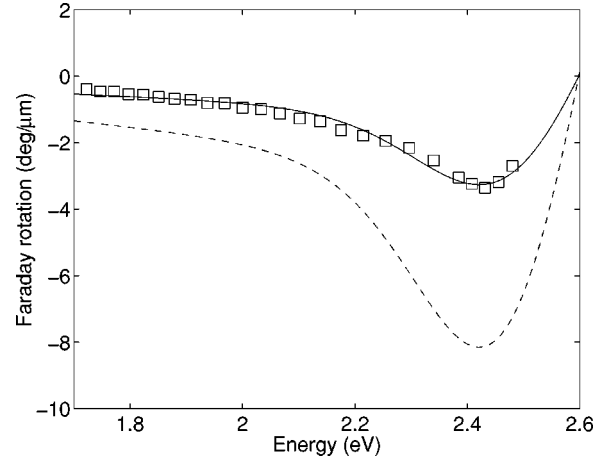


FIG. 2. The Faraday rotation as a function of wavelength for sample 8. The dashed line shows the predicted Faraday rotation for $x=1.5$ and $z=0.9$.

For $x < 2$ it is reasonable to assume that N is directly proportional to the bismuth content x .²³ Furthermore, it is known that the strong enhancement of Faraday rotation is caused by iron-pair transitions, involving both octahedral and tetrahedral transitions simultaneously.²⁵ Therefore iron dilution of either sublattice results in a reduction of the active ion density. For these reasons we assume that the active ion density can be written as²³

$$N = N_0(1 - z_d/3)(1 - z_a/2)x. \quad (2)$$

N_0 is a constant, and may be expected to be 1/3 of the density of rare-earth ions on the dodecahedral site, i.e., $1.3 \times 10^{22} \text{ cm}^{-3}/3$. When $x=3$, this interpretation implies that the dodecahedral site is fully occupied by bismuth.

To fit theoretical curves to the experimental data, the product $N_0 f_i$ was chosen as free parameter. The parameters Δ_i , ω_i , and Γ_i were chosen as sample independent, and the values suggested in Ref. 23 were used as a starting point in the fitting. Table II presents the parameters found to give the best fit between the theoretical curves and experimental data. Note that our values for Δ_i , ω_i , and Γ_i differs slightly from those used in Ref. 23. This is due to the fact that in that paper we focused on obtaining a very good fit for energies less than 2.3 eV. However, this resulted in some deviations between experiment and theory near the maximum Faraday rotation. Here we have chosen parameters which give the best agreement within the whole range of experimental data.

TABLE II. The parameters found to give the best fit between Eq. (1) and the experimental data. Note that the tetrahedral and octahedral sites are given different signs, since they contribute oppositely to the Faraday rotation.

Site	$N_0 f_i \text{ (cm}^{-3}\text{)}$	$\Delta_i \text{ (eV)}$	$\omega_i \text{ (eV)}$	$\Gamma_i \text{ (eV)}$
a	2.2×10^{23}	0.4	3.10	0.5
d	-6.4×10^{22}	0.1	2.47	0.3

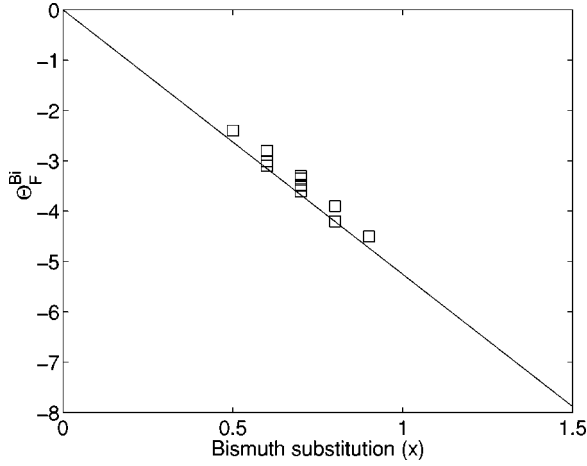


FIG. 3. Θ_F^{Bi} ($^{\circ}/\mu\text{m}$) as a function of bismuth substitution at 2.3 eV. The solid line is the theoretical curve obtained using Eq. (1).

The solid line shown in Fig. 1 is the Faraday rotation calculated from Eq. (1) using the values in Table II. The dashed and dash-dotted lines show the contribution to the total Faraday rotation from the octahedral and tetrahedral sites, respectively. Note that below 2.2 eV, the main contribution to Θ_F comes from the octahedral site.

The solid line in Fig. 2 shows the calculated Faraday rotation of sample 8. Again, we note that the theoretical curve is in good agreement with the experimental data. Also shown is the theoretical predictions when the bismuth content is $x = 1.5$ (dashed line). In this case one may expect almost $7^{\circ}/\mu\text{m}$ at 2.3 eV.

It is useful to find out how bismuth and gallium influence the Faraday rotation. To this end, we define the following parameters:

$$\Theta_F^{Bi} = \frac{\Theta_F^{sat}}{(1 - z_d/3)(1 - z_a/2)} \quad (3)$$

and

$$\Theta_F^{Ga} = \frac{\Theta_F^{sat}}{x}. \quad (4)$$

Here Θ_F^{Bi} and Θ_F^{Ga} are the Faraday rotations associated with the bismuth and gallium content, respectively. The experimental data and theoretical curves for these two parameters are plotted in Figs. 3 and 4, respectively. The good agreement between experimental data and theoretical predictions confirm the validity of the model used here.

IV. SENSITIVITY

If a light beam propagates along the z axis through the magnetic film, then the polar Faraday rotation of the film is given by (neglecting the Voigt-effect and multiple reflections)¹⁷

$$\Theta_F = \Theta_F^{sat} \frac{H_z}{H_a}, \quad H_z \leq H_a, \quad (5)$$

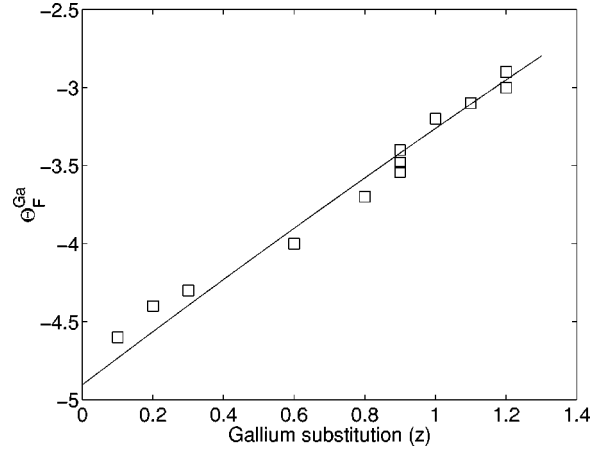


FIG. 4. Θ_F^{Ga} ($^{\circ}/\mu\text{m}$) as a function of gallium substitution at 2.3 eV. The solid line is the theoretical curve obtained using Eq. (1).

where the anisotropy field is defined by

$$H_a = M_s - \frac{2K_u^{tot}}{\mu_0 M_s}. \quad (6)$$

We have here assumed that the thicknesses of the films are much smaller than any lateral dimensions, which means that shape anisotropy can be approximated by that of a thin film of infinite extent. Equation (5) is only valid as long as the cubic anisotropy can be neglected. When $H_z \geq H_a$, the Faraday rotation is at its maximum value. As an example, the Faraday rotation as a function of H_z for sample 4 is shown in Fig. 5. Note that the Faraday rotation is accurately described by Eq. (5) as long as $H_z < H_a$. In Fig. 6 the experimental values for H_a is displayed as a function of gallium substitution. The dashed line shows the best fit to H_a for films with composition $\text{Lu}_{3-x}\text{Bi}_x\text{Fe}_{5-z}\text{Ga}_z\text{O}_{12}$,

$$H_a \approx 210\,000(1 - 0.7z). \quad (7)$$

Also shown is the value for M_s found in the literature,^{5,6,26}

$$M_s \approx 160\,000(1 - 0.75z). \quad (8)$$

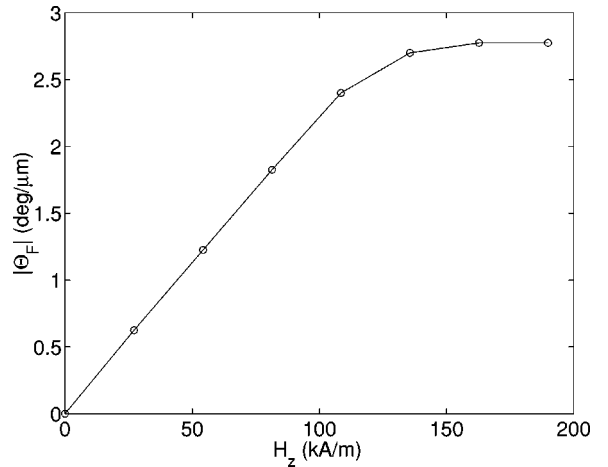


FIG. 5. The Faraday rotation as a function of H_z for sample 4 for a photon energy of 2.3 eV.

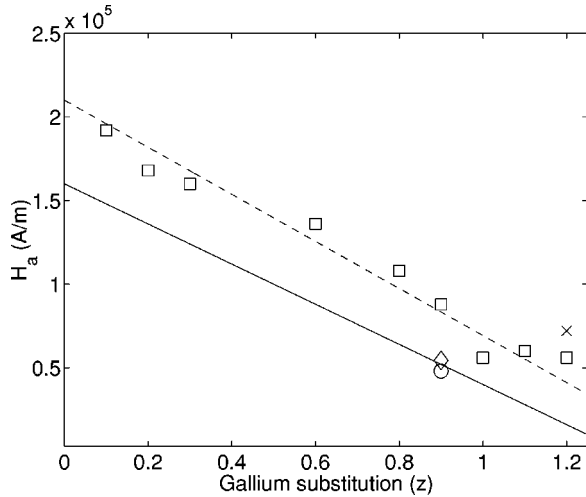


FIG. 6. The saturation field as a function of gallium substitution.

The experimental values for H_a are quite close to Eq. (8), which indicates that the uniaxial anisotropy plays a minor role here. Since the films of composition $\text{Lu}_{3-x}\text{Bi}_x\text{Fe}_{5-z}\text{Ga}_z\text{O}_{12}$ are well described by Eq. (7), we will use this in the further modelling. Films 7, 8, and 12 are not well described by Eq. (7), which is most probably due to the fact that they contain thulium or yttrium ions on the dodecahedral sites. The Faraday rotation sensitivity is given by

$$S = \frac{d\Theta_F}{dH_z} = \frac{\Theta_F^{sat}}{H_a}. \quad (9)$$

It is useful to separate the contributions from bismuth and gallium. The contribution from bismuth can be written as

$$S^{Bi} = \frac{S(1-0.7z)}{(1-z_d/3)(1-z_a/2)}. \quad (10)$$

The experimental data points at 2.3 eV (wavelength 540 nm) are shown in Fig. 7 together with the theoretical prediction based on Eq. (10). A reasonably good agreement is obtained for all samples of composition $\text{Lu}_{3-x}\text{Bi}_x\text{Fe}_{5-z}\text{Ga}_z\text{O}_{12}$, ex-

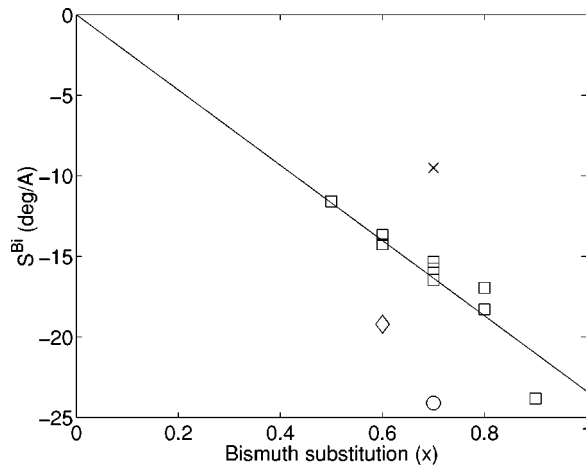


FIG. 7. The sensitivity as a function of bismuth substitution for a photon energy of 2.3 eV.

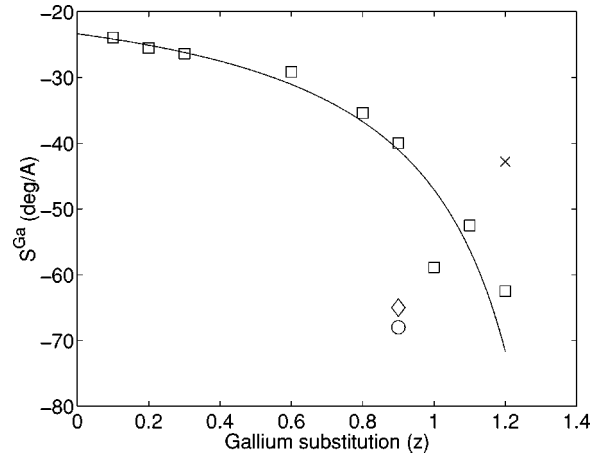


FIG. 8. The sensitivity as a function of gallium substitution for a photon energy of 2.3 eV.

cept sample 11, which shows a minor deviation from the theoretical curve. We do not know the reason for this deviation. It is interesting to observe that the sensitivity depends linearly on the bismuth content. The experimental data for samples 7, 8, and 12 (diamond, circle, and cross) are located far from the straight line, since they do not follow Eq. (7).

It is also of interest to see how gallium influences the sensitivity of the material. To that end, we define

$$S^{Ga} = \frac{S}{x}. \quad (11)$$

In Fig. 8 the experimental data points are shown together with the theoretical prediction based on Eq. (11). Again we note that there is good agreement between the experimental data and the theoretical curve for samples of composition $\text{Lu}_{3-x}\text{Bi}_x\text{Fe}_{5-z}\text{Ga}_z\text{O}_{12}$ (except for sample 11, which shows a minor deviation from the theoretical curve). Now the sensitivity has a strong nonlinear dependence on the gallium content. Thus one may think that it should be possible to increase the sensitivity even further by adding more gallium. However, this is not the case. If we add more gallium (above $z=1.2$), the film approaches its compensation point ($M_s=0$) where the coercivity of the material is rather high. On the other hand, it would be of interest to investigate the sensitivity above the compensation point, but this is outside the scope of this paper.

V. CONCLUSION

We have investigated the Faraday rotation of in-plane magnetized bismuth-substituted ferrite garnet films grown by liquid phase epitaxy on (100) oriented gadolinium gallium garnet substrates. The Faraday spectra were measured for photon energies between 1.7 and 2.6 eV. To interpret the spectra, we use a simple model based on two electric dipole transitions, and find excellent agreement with the experimental data. Furthermore, the Faraday rotation sensitivity was

measured at 2.3 eV, and found to be in good agreement with the theoretical predictions. In particular, we find that the sensitivity increases linearly with the bismuth content and nonlinearly with the gallium content.

ACKNOWLEDGMENTS

This work was financially supported by The Norwegian Research Council and Tandberg Data ASA.

-
- ¹S. Wittekoek and D.E. Lacklison, *Phys. Rev. Lett.* **28**, 740 (1972).
²S. Wittekoek, T.J.A. Popma, J.M. Robertson, and P.F. Bongers, *Phys. Rev. B* **12**, 2777 (1975).
³H. Takeuchi, *Jpn. J. Appl. Phys., Part 1* **14**, 1903 (1975).
⁴G.S. Krinchik, V.A. Krylova, E.V. Beredennikova, and R.A. Petrov, *Sov. Phys. JETP* **38**, 354 (1974).
⁵P. Hansen, M. Rosenkrantz, and K. Witter, *Phys. Rev. B* **25**, 4396 (1982).
⁶P. Hansen, C.P. Klages, J. Schuldt, and K. Witter, *Phys. Rev. B* **31**, 5858 (1985).
⁷P. Hansen, K. Witter, and W. Tolksdorf, *J. Appl. Phys.* **55**, 1052 (1984).
⁸P. Hansen, K. Witter, and W. Tolksdorf, *Phys. Rev. B* **27**, 6608 (1983).
⁹Z. Simsa, J. Simsova, D. Zemanova, J. Cermak, and M. Nevřiva, *Czech. J. Phys.* **34**, 1102 (1984).
¹⁰A.I. Belyaeva, A.L. Foshchan, and V.P. Yur'ev, *Pis'ma Zh. Tekh. Fiz.* **17**, 76 (1991) [*Sov. Tech. Phys. Lett.* **17**, 599 (1991)].
¹¹L.A. Dorosinskii, M.V. Indenbom, V.I. Nikitenko, Y.A. Ossip'yan, A.A. Polyanskii, and V.K. Vlasko-Vlasov, *Physica C* **203**, 149 (1992).
¹²M.R. Koblischka and R.J. Wijngaarden, *Supercond. Sci. Technol.* **8**, 199 (1995).
¹³V.K. Vlasko-Vlasov, Y. Lin, U. Welp, G.W. Crabtree, D.J. Miller, and V.I. Nikitenko, *J. Appl. Phys.* **87**, 5828 (2000).
¹⁴A. Hubert and R. Schafer, *Magnetic Domains*, 1st ed. (Springer-Verlag, Berlin, 1998).
¹⁵A.N. Egorov and S.V. Lebedev, *J. Appl. Phys.* **87**, 5362 (2000).
¹⁶A. Zvezdin and V. Kotov, *Modern Magneto-optics and Magneto-optical Materials* (IOP Publishing, Bristol, 1997).
¹⁷M. Shamonin, M. Klank, O. Hagedorn, and H. Dötsch, *Appl. Opt.* **40**, 3182 (2001).
¹⁸M.N. Deeter, A.H. Rose, G.W. Day, and S. Samuelson, *J. Appl. Phys.* **70**, 6407 (1991).
¹⁹M.N. Deeter, S.M. Bon, G.W. Day, G. Diercks, and S. Samuelson, *IEEE Trans. Magn.* **30**, 4464 (1994).
²⁰M.N. Deeter and S.M. Bon, *Appl. Phys. Lett.* **69**, 702 (1996).
²¹I.M. Syvorotka, S.B. Ubizskii, M. Kucera, M. Kuhn, and Z. Vertesy, *J. Phys. D* **34**, 1178 (2001).
²²M. Wallenhorst, M. Niemöller, H. Dötsch, P. Hertel, and B. Gather, *J. Appl. Phys.* **77**, 2902 (1995).
²³L.E. Helseth, R.W. Hansen, E.I. Il'yashenko, M. Baziljevich, and T.H. Johansen, *Phys. Rev. B* **64**, 174406 (2001).
²⁴E.R. Czerlinsky, *Phys. Status Solidi* **34**, 483 (1969).
²⁵G.B. Scott, D.E. Lacklison, and J.L. Page, *J. Phys. C* **8**, 519 (1975).
²⁶V.J. Fratello, S.E.G. Slusky, C.D. Brandle, and M.P. Norelli, *J. Appl. Phys.* **60**, 718 (1986).
²⁷G.F. Dionne and G.A. Allen, *J. Appl. Phys.* **75**, 6372 (1994).
²⁸G.F. Dionne and G.A. Allen, *J. Appl. Phys.* **73**, 6127 (1993).